

Nuclear magnetic cooling to 1.6 mK and nuclear ferromagnetism in PrTl_3

K. Andres and S. Darack

Bell Laboratories, Murray Hill, New Jersey 07974

(Received 4 April 1974)

Details of hyperfine enhanced nuclear-magnetic-cooling experiments to 1.6 mK with the Van Vleck paramagnetic compound PrTl_3 are given. Measurements of the nuclear specific heat and the hyperfine enhanced nuclear magnetic susceptibility in this very-low-temperature range are presented which extrapolate to a nuclear ferromagnetic ordering temperature of 1.0 ± 0.3 mK.

I. INTRODUCTION

We have shown before¹⁻⁶ that many intermetallic praseodymium compounds are suitable for nuclear-magnetic-cooling experiments. In such compounds, the crystal-field ground state of the Pr ion is a singlet and the crystal-field splitting is rather small, leading to large Van Vleck susceptibilities. Application of an external field at low temperatures then results in the generation of rather large hyperfine fields at the Pr nucleus, typically of order 10 to 20 times the applied field. These fields can be used conveniently to polarize Pr nuclei at temperatures around 30 mK and to cool the sample to much lower temperatures by adiabatic demagnetization. In PrTl_3 , the hyperfine field is initially 17.3 times the applied field (equal to the hyperfine enhancement factor), and adiabatic cooling yields end temperatures around 1.6 mK. In this paper we present nuclear-specific-heat and nuclear-susceptibility measurements on PrTl_3 down to these low temperatures, which suggest that the Pr-nuclei undergo ferromagnetic order at 1.0 ± 0.3 mK.

II. EXPERIMENTAL

Magnetic-susceptibility measurements above 1 K were carried out in a dc magnetometer, the principle of which is described elsewhere.^{7,8} A ^3He - ^4He dilution refrigerator was used for the demagnetization experiments. To reduce heat leaks into the adiabatically suspended sample, the whole cryostat is hung from a heavy hardwood table which is supported pneumatically on a steel frame and located inside an electrically shielded room. The dilution refrigerator has only one continuous concentric tube type heat exchanger. To reduce eddy current heating, the mixing chamber is made out of brass; it reaches lowest temperatures of about 25 mK. Details of the sample suspension are shown in Fig. 1. The PrTl_3 sample (of cylindrical shape, 0.58 cm in diameter and 4.4 cm long) is located in the tail section of the cryostat in the center of a superconducting solenoid. It is connected thermally to the mixing chamber via a strand of about 3000 No. 40 Formex insulated Cu wires, with

a superconducting (SC) thermal switch (made out of tin, $0.15 \times 0.15 \times 0.15$ cm) in series. The latter is operated with a small niobium solenoid in the high-vacuum space. Below the PrTl_3 sample, a cylindrical piece of the compound AuIn_2 is situated at the center of a smaller superconducting solenoid. This AuIn_2 probe serves as a nuclear-susceptibility thermometer⁹; it is connected to the PrTl_3 sample again by a Cu-wire strand. Solder connections are made with pure cadmium metal. Top and bottom connections at the PrTl_3 sample are made such that the Cu-wire strand is first silver soldered to Cu-cups, which then are Cd soldered to the PrTl_3 ends. This latter operation had to be done in a vacuum on a freshly cleaned sample, since PrTl_3 oxidizes rather rapidly in air. Three heat shields surround the sample and the thermometer; they

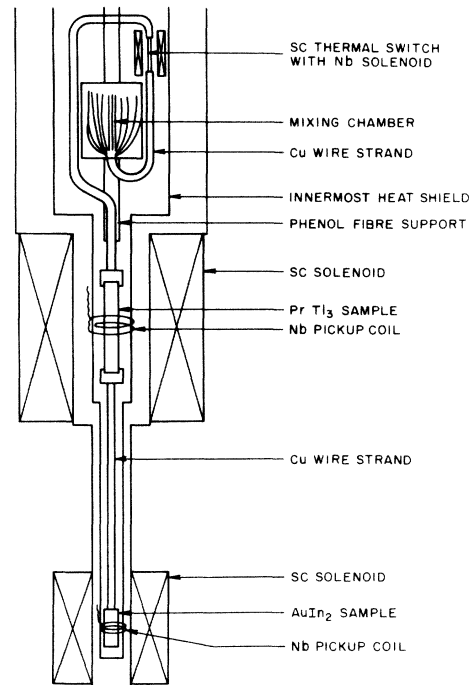
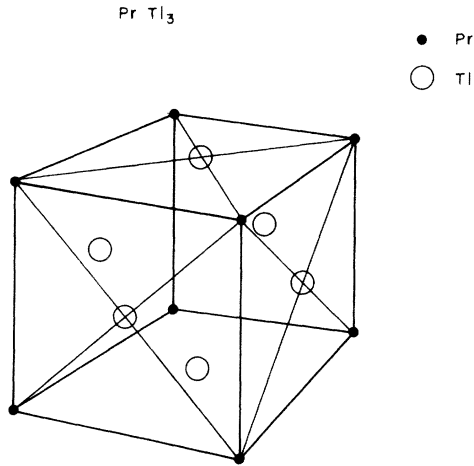


FIG. 1. Demagnetization apparatus.

FIG. 2. Unit cell of PrTl₃.

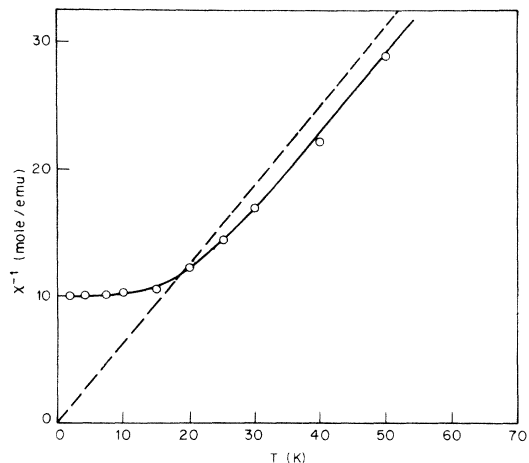
are made out of copper coil foil and are thermally anchored, respectively, to the 1° plate, the continuous exchanger (~0.2K), and the mixing chamber. To measure the magnetization of both the PrTl₃ sample and the AuIn₂ thermometer, two niobium pickup coils (8 turns each) are wound around the innermost heat shield, centered in each magnet. They each form the primary of a superconducting transformer, the secondary being located outside the vacuum can in a lead superconducting shield. Changes in magnetization are then monitored with flux-gate magnetometer probes operating in liquid helium, as described before.^{6,8} A high field stability in the superconducting solenoids is required for the magnetization measurements, especially immediately after demagnetization from high fields. This was achieved by winding two one-layer SC coils inside the solenoid bore, the first one (in two sections) for shielding out field drifts at the ends of the solenoid and another for stabilizing the field in its center section (the two persistent current switches for these auxiliary coils are operated simultaneously with the main persistent current switch). Temperatures down to 30 mK are measured with a cerium magnesium nitrate thermometer as described in Ref. 6 as well as with carbon resistance thermometers. Below 30 mK, temperatures are measured with the AuIn₂ nuclear-susceptibility thermometer as described in Ref. 8.

Samples of PrTl₃ were prepared by first pre-reacting chips of the material for one day at 900 °C in sealed off Ta crucibles and then melting them (in the same crucibles) in a vacuum furnace. It was found that when melting was done with the crucible (0.635 cm in diameter, 10 cm long) in a vertical position, the sample homogeneity was poor (Pr rich at the top and Tl rich at the bottom). Attempts to improve the homogeneity by zone refining

samples made in this way were unsuccessful. Melting was then done with the crucible in a horizontal position and with an arrangement whereby it could be tilted up and down in order to agitate the molten samples. Samples made in this way were quite homogeneous but still not purely single phase since they always contained a small volume fraction (~1%) of free thallium metal. Attempts to suppress this by starting with slightly off stoichiometric (Pr-rich) samples were unsuccessful. Although traces of free Tl metal will not alter significantly the magnetic properties of PrTl₃ in fields above 160 Oe, such traces may introduce irreversible heat in demagnetization experiments when the field is reduced below 160 Oe (the superconducting critical field of Tl).

III. MAGNETIC PROPERTIES OF PrTl₃ ABOVE 1 K

PrTl₃ crystallizes in the Cu₃Au structure (Fig. 2). Each Pr ion is surrounded by 12 nearest Tl neighbors in cubic symmetry. Assuming a positive point charge on the Tl ions [it should be mentioned here that in the compound Pr₃Tl, which is a singlet-ground-state (or induced-moment) ferromagnet,^{9,10} and which crystallizes in the same structure, a positive charge had to be assigned also to both the Pr and Tl ions to explain the magnetic and thermodynamic properties in the point-charge model], the crystal-field calculations by Lea, Leask, and Wolf¹¹ would predict a singlet crystal-field ground state for the ³H₄ multiplet ($L=5$, $S=1$, $J=4$) of the Pr³⁺ ion, the next higher state being a triplet. In agreement with this, PrTl₃ is found to be Van Vleck paramagnetic at low temperatures, as shown by the susceptibility measurements of Fig. 3. The Van Vleck susceptibility below 4 K is found to be

FIG. 3. Inverse magnetic susceptibility of PrTl₃ between 1 and 50 K.

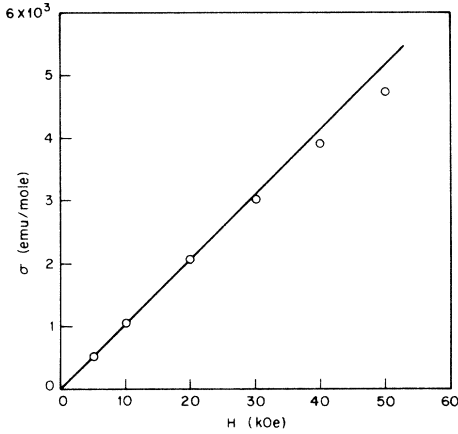


FIG. 4. Molar magnetic moment of PrTl_3 versus applied field at 1.2 K.

$$\chi_{\text{VV expt}} = 0.10 \pm 0.005 \text{ emu/mole.} \quad (1)$$

The field dependence of the Van Vleck moment at 1.2 K is shown in Fig. 4. χ_{VV} is seen to be nearly field independent up to 30 kOe, where it has decreased by 2.6% from its zero-field value. Since the Van Vleck susceptibility arises from an admixture of the next triplet state into the ground state (this state having the only nonvanishing matrix element of angular momentum with the ground state), this means that the triplet state cannot lie too close to the ground state. Specific-heat measurements in the helium temperature range show a Schottky-type contribution, which is compatible with a next-higher-lying triplet state at 37 K above the ground state.⁹ We can then compare the result (1) with the theoretically expected crystal-field susceptibility, which is given by

$$\chi_{\text{CF}} = 2g^2 \mu_B^2 \alpha^2 / \Delta = 0.0866 \text{ emu/mole.} \quad (2)$$

Here $\alpha = \sqrt{20/3}$ is the matrix element of angular momentum between the ground state and the first triplet state. The fact that $\chi_{\text{VV expt}}$ is somewhat larger than the crystal-field susceptibility can be explained by the presence of ferromagnetic exchange interactions. In molecular-field approximation, the exchange enhancement is given by

$$\chi_{\text{VV}} = \frac{\chi_{\text{CF}}}{1 - \lambda \chi_{\text{CF}}} \quad (3)$$

and we would need $\lambda \chi_{\text{CF}} = 0.13 \pm 0.04$ to explain the observed Van Vleck susceptibility. PrTl_3 is thus far from being a critical singlet-ground-state system where the critical parameter $\lambda \chi_{\text{CF}}$ would be close to 1 (such as is the case, e.g., in $\text{Pr}_3\text{Tl}^{10,12}$). The hyperfine field, which is induced at the Pr nuclei via the Van Vleck moment, is proportional to

χ_{VV} and given by

$$H_{\text{hf}} = H_{\text{ext}} + h_f \chi_{\text{VV}} H_{\text{ext}}, \quad (4)$$

with

$$h_f = A / (g_N g_J \mu_N \mu_B L) = 187.7 \text{ mole/emu,}$$

or, with the definition $K = h_f \chi_{\text{VV}}$,

$$H_{\text{hf}} = (1 + K) H_{\text{ext}}. \quad (4')$$

The values used to compute h_f are $g_N = 1.71$, $g_J = 0.8$, $A/k = 0.0525 \text{ K}$, and $L = 6.03 \times 10^{23}$. With the value $\chi_{\text{VV}} = 0.10 \pm 0.005 \text{ emu/mole}$, the hyperfine enhancement $1 + K$ of the local field at the Pr nuclei over the external applied field is thus 19.8 ± 1 .

IV. MAGNETIC AND THERMODYNAMIC PROPERTIES OF PrTl_3 BELOW 1 K

The induced hyperfine field gives rise to a Zeeman splitting of the six nuclear substates of the singlet ground state (the nuclear-spin quantum number I of ^{141}Pr is $\frac{5}{2}$). This splitting is given by

$$E_N = -g_N \mu_N I_z H(1 + K); \quad (5)$$

it in turn gives rise to a Curie-like nuclear magnetic susceptibility of the form

$$\chi_N(\text{per mole}) = \frac{C_N}{T} = \frac{L g_N^2 \mu_N^2 I(I+1)(1+K)^2}{3kT}. \quad (6)$$

This nuclear susceptibility is superimposed on the (temperature-independent) Van Vleck susceptibility. Because of its large hyperfine enhancement $(1+K)^2$, it becomes observable below 1 K. Figure 5 is a plot of χ_N versus T^{-1} (where χ_N is the observed increase of the total susceptibility over the Van Vleck value) in the temperature range between 0.5 K and 10 mK. We observe indeed a Curie law with a Curie constant (per mole) of $2.84 \times 10^{-4} \text{ cm}^3 \text{ K}$. Using Eq. (6) (with $I = \frac{5}{2}$ and $g_N = 1.71$) we deduce from this value a hyperfine enhancement factor $1 + K$ of 17.3, in fair agreement

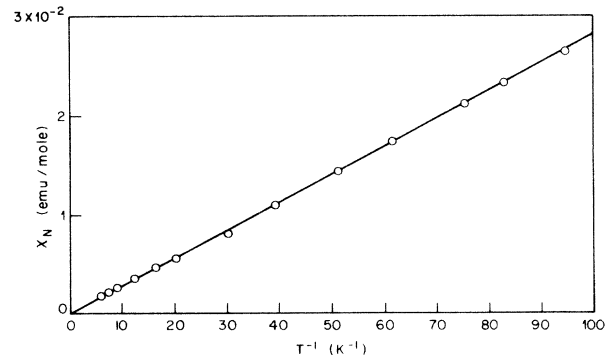


FIG. 5. Hyperfine enhanced nuclear magnetic susceptibility of PrTl_3 below 0.5 K, plotted versus $1/T$.

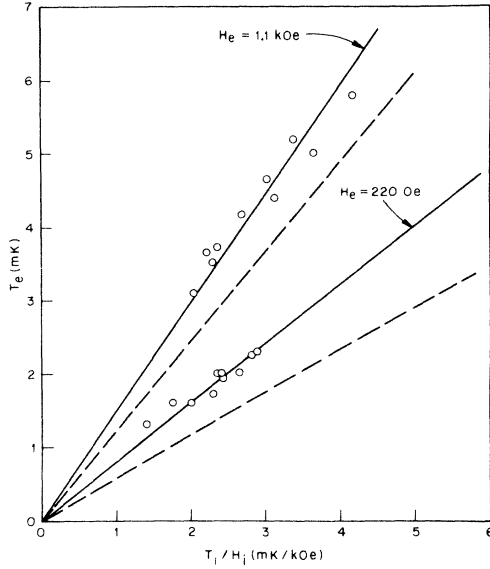


FIG. 6. Observed end temperatures after demagnetizations as a function of different starting conditions T_i and H_i for two end fields (220 and 1100 Oe).

with the value of 19.8 deduced before from χ_{VV} .

Temperatures below 30 mK were obtained by adiabatic demagnetization of the sample. Demagnetizations were carried out in fields of up to 25.7 kOe and from starting temperatures between 30 and 60 mK. Residual fields of 147, 367, 917, and 1836 Oe were left on the sample and the magnetic-susceptibility change on warming up was recorded as a function of temperature. As long as the Pr nuclei remain paramagnetic, i. e., their entropy and magnetization is only a function of H/T , the temperature T_e after isentropic demagnetization should be given by

$$T_e = (T_i/H_i)H_e. \quad (7)$$

Equation (7) can be generalized to include an exchange or dipolar field of magnitude $H_0(1+K)$ acting on the nuclei in molecular-field approximation. It then reads

$$T_e = (T_i/H_i)(H_e^2 + H_0^2)^{1/2}. \quad (8)$$

Figure 6 is a plot of observed end temperatures as a function of starting conditions T_i/H_i for two different end fields (1.1 kOe and 220 Oe). The data do indeed roughly follow Eq. (8), except that from the slopes of the two lines (for 1.1 and 0.22 kOe) one would extract two different values of H_0 , namely, 989 and 775 Oe, respectively. However, we have observed that our demagnetizations do not occur isentropically, which means that the data in Fig. 6 and the values of H_0 extracted from it have only empirical value. A much better determination of H_0 is possible by specific-heat mea-

surements (see below) and yields 534 Oe. Using this value, the ideal end temperatures (without entropy loss) as a function of T_i/H_i for the two end fields 1.1 and 0.22 kOe would lie closer to the two dashed lines in Fig. 6. We have determined experimentally the entropy loss by first demagnetizing to the end field and then remagnetizing to exactly the starting temperature. The field at this latter stage is always lower than the initial starting field and is a measure of the total entropy loss. The ideal nuclear-cooling entropy, calculated according to

$$\begin{aligned} \frac{S}{R} = & \ln(2I+1) - (x/2) \coth(x/2) \\ & + \frac{1}{2}(2I+1)x \coth[(2I+1)x/2] \\ & - \ln \frac{\sinh[(2I+1)x/2]}{\sinh(x/2)}, \end{aligned} \quad (9)$$

with

$$x = g_N \mu_N H(1+K)/kT, \quad 1+K = 17.3$$

is plotted in Fig. 7 as a function of H_i/T_i (we have never used fields above 30 kOe and have neglected the small field dependence of χ_{VV} below 30 kOe). It can be seen that for our best starting conditions ($H_i = 25.7$ kOe, $T_i = 36$ mK), a rather large amount (31.7%) of the total nuclear-cooling entropy is extracted, thanks to the large hyperfine field enhancement. To reach this latter starting condition, the sample, which weighed 12.1 g (1.60×10^{-2} mole of Pr) had to be precooled for about $2\frac{1}{2}$ h. Figure 8 shows the observed entropy loss during demagnetization for a number of experiments. Plotted on the x axis is the ideal cooling entropy (obtained from H_i/T_i and Fig. 7), and on the y axis the actu-

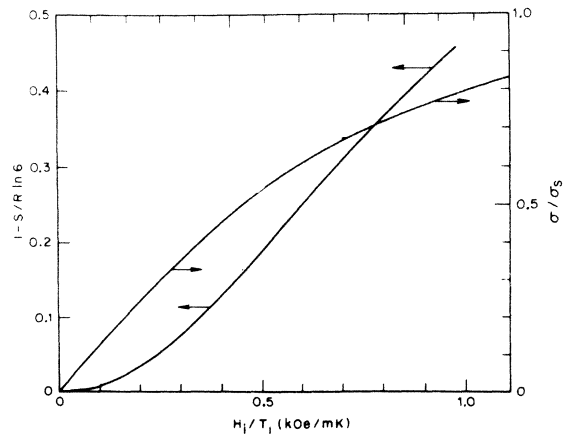


FIG. 7. Nuclear-cooling entropy and hyperfine-enhanced nuclear magnetization as a function of the starting condition H_i/T_i .

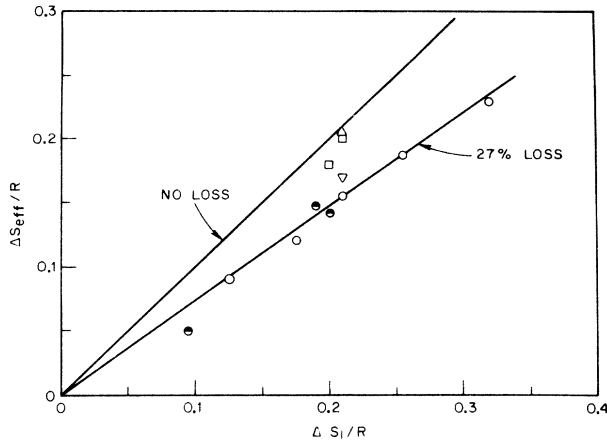


FIG. 8. Ideal cooling entropy (abscissa) versus observed cooling entropy (ordinate) for different demagnetizations (see text). The different points distinguish the different end fields used: Δ , 14.7 kOe; \square , 11 kOe; ∇ , 3.67 kOe; \bullet , 1.1 kOe; \circ , 183 Oe.

ally available cooling entropy (we have assumed that the entropy loss is the same on demagnetizing and remagnetizing). When demagnetizing to fields less than about 1000 Oe, the entropy loss is roughly proportional to the initial cooling entropy and of order 20–30% in magnitude. This loss was independent of the field sweep time for demagnetization times longer than 5 min; it was somewhat larger for faster demagnetizations. In all demagnetizations shown in Fig. 8 the end field was kept above 160 Oe (the SC critical field of the thallium traces in our sample). At present we do not know the actual source of this irreversibility.

A. Susceptibility below 10 mK

The lowest temperature reached in an end field of 147 Oe was 1.6 mK. The inverse of the nuclear susceptibility (the latter determined as before by subtracting χ_{VV} from the total susceptibility) is plotted against temperature for different fields in Fig. 9. From 10 down to 1.6 mK and in fields below 367 Oe, χ_N follows a Curie-Weiss law with a Curie constant of 2.84×10^{-4} emuK/mole and a Curie-Weiss temperature $\Theta = 1.0 \pm 0.3$ mK. The data below 10 mK then can be well represented by a modification of Eq. (6), which reads

$$\chi_N = \frac{\chi_N^0}{1 - \lambda' \chi_N^0} = \frac{C_N^0}{T - \Theta}, \quad (10)$$

$$\Theta = \lambda' C_N^0, \quad (11)$$

and is the usual molecular-field formula for the susceptibility of exchange-coupled moments. Here χ_N^0 is the hyperfine enhanced nuclear susceptibility far from the nuclear ordering temperature and $\lambda' = \lambda[K/(1+K)]^2$ (λ is the usual molecular-field exchange constant). From the previously determined

value of $\lambda\chi_{CF} = 0.13 \pm 0.4$ [Eq. (3)] we can compute, according to Eq. (11), a Curie-Weiss temperature $\Theta = \lambda\chi_{CF}[K/(1+K)]^2 C_N^0/\chi_{CF}$ of 0.39 ± 0.12 mK, somewhat lower than the value extrapolated from Fig. 9. Equations (6) and (10) should be valid when the hyperfine splitting of the nuclear substates in the singlet ground state can be treated as a second-order perturbation, i.e., when $A/\Delta \ll 1$ and $\lambda\chi_{CF} \ll 1$. A better treatment of the combined electron-nuclear system has been given in Ref. 13. This would predict, again with $\lambda\chi_{CF} = \eta = 0.13 \pm 0.4$ [Eq. (24) of Ref. 13], an ordering temperature of 0.50 ± 0.17 mK and characterizes the order as being of the cooperative nuclear type (as opposed to the induced-moment order which one would expect for values of $\lambda\chi_{CF}$ larger than 0.62). Thus the predicted ordering temperature comes within a factor of about 2 of what we extrapolate from Fig. 9, which is probably as good an agreement as can be expected from a simple molecular-field treatment. The highest observed hyperfine enhanced nuclear moment (at 1.6 mK in 367 Oe) was 131 emu/mole. This can be compared with the saturation moment (the moment of the lowest nuclear substate), which in second-order perturbation theory is given by

$$\begin{aligned} \langle m_0 \rangle &= (2A\alpha^2/\Delta) I g_J \mu_B + g_N \mu_N I \\ &= 211 + 13 = 224 \text{ emu/mole.} \end{aligned} \quad (12)$$

The first term on the right-hand side of Eq. (12) is the $4f$ angular momentum that the hyperfine interaction $A\mathbf{J} \cdot \mathbf{I}$ admixes to the nuclear substates in the singlet ground state ($A/k = 0.052$ K, $\alpha^2 = \frac{20}{3}$, $\Delta/k = 37$ K, $g_J = 0.8$, $g_N = 1.71$, $I = \frac{5}{2}$). The highest observed nuclear polarization was thus 58.5% of the saturation value. This can be compared to the initial polarization computed from H_i/T_i : To reach 1.6 mK in 367 Oe we used $H_i = 25.7$ kOe and T_i

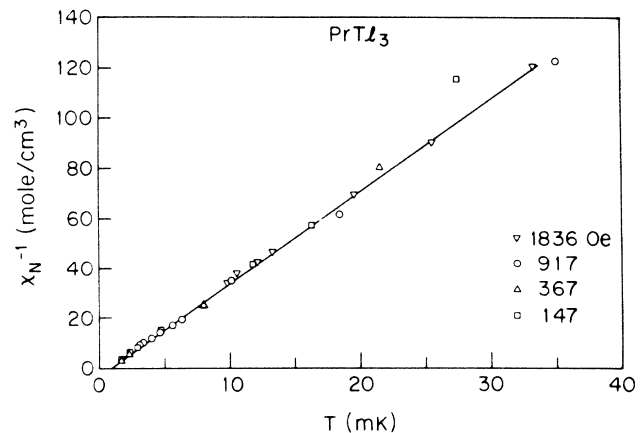


FIG. 9. Inverse hyperfine enhanced nuclear magnetic susceptibility of PrTl_3 below 40 mK in different applied fields.

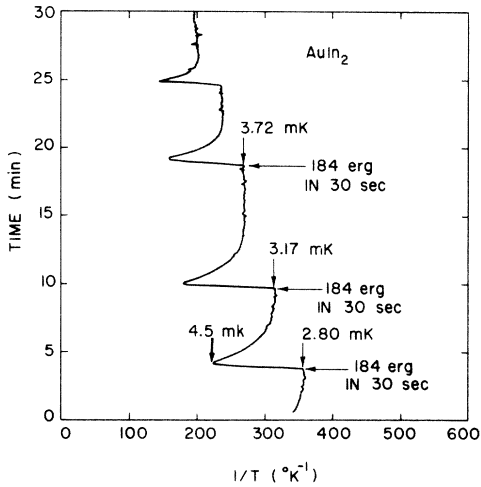


FIG. 10. Temporal response of the AuIn_2 nuclear-susceptibility thermometer to heat pulses (see text).

= 36 mK which gives a cooling entropy (Fig. 7) of 31.7% of $R \ln 6$. Subtracting a loss of 25% from this, we obtain 23.8% of actual cooling entropy. According to the Brillouin function (which is also shown in Fig. 7), the magnetization corresponding to this entropy is of 60% of saturation. This is in agreement with the observed 58.5% at low temperatures and says that the magnetization does not change during an isentropic demagnetization. Thermodynamically, this is to be expected as long as one stays in the paramagnetic regime above the ordering temperature, where both the entropy and the magnetization are only functions of $x = g\mu_B(H^2 + H_0^2)^{1/2}/kT$ (H_0 is the exchange field).

B. Specific-heat measurements below 20 mK

Specific-heat measurements were carried out simultaneously with the susceptibility measurements by warming up the sample with heat pulses after the demagnetization. Two similar heater coils ($\sim 300 \Omega$ each) made out of Manganin wire were wrapped around the Cu-wire strands on both sides of the PrTl_3 sample, the heat contact being made by Apiezon grease. A typical response of the AuIn_2 thermometer to heat pulses is shown in Fig. 10. It can be seen that the AuIn_2 signal responds quickly to the pulses but that the PrTl_3 sample itself has a much larger thermal relaxation time. This is due entirely to the large nuclear specific heat and the relatively low thermal conductivity of PrTl_3 at these low temperatures. Rough measurements of the thermal conductivity of PrTl_3 at 55 mK give a value of 3.7 mW/cmK in zero field. With a residual resistivity of $6.35 \times 10^{-7} \Omega \text{ cm}$ (at 4.2 K) this gives a Lorentz number of 0.427

$\times 10^{-7} (V/K)^2$, almost twice the ideal value of $0.244 \times 10^{-7} (V/K)^2$. At the lowest temperatures, the specific heat C/R (per mole) reaches values of about 0.6, which would give thermal relaxation times of order

$$\tau_{\text{th}} = Cl^2/V_m \lambda = 4.5 \text{ min} \quad (13)$$

(V_m is the molar volume, l the length of sample), in agreement with our observations. The nuclear spin-lattice relaxation time is presumably very much shorter than that. The specific-heat data in different fields are shown in Fig. 11 in a doubly logarithmic plot of C/R versus T . The accuracy of the data at the low-temperature end is limited both because of the long thermal relaxation times as well as because of residual heat leaks into the sample which were usually between 3 and 6 erg/min. In the higher fields, the specific heat clearly varies as $1/T^2$ (straight lines in Fig. 11), as expected for the high-temperature part of a nuclear Schottky-type anomaly. It should be given, according to thermodynamics, by

$$C/R = C_N(H_e^2 + H_0^2)/RT^2, \quad (14)$$

where C_N is the Curie constant (per mole) of Eq. (6). In the lower fields, there is no clearcut $1/T^2$ region any more, and the specific heat rises faster at the lowest temperatures. This signals the approach of a phase transition. Unfortunately, our measurements do not extend below the ferromagnetic ordering temperature. This would of

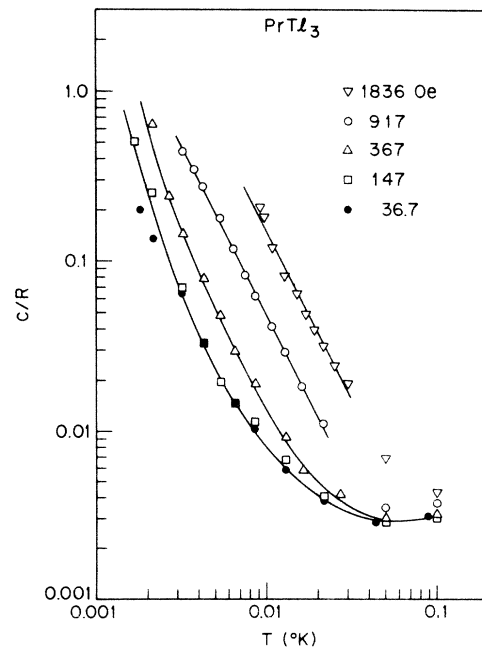


FIG. 11. Molar specific heat of PrTl_3 below 0.1 K in different applied fields.

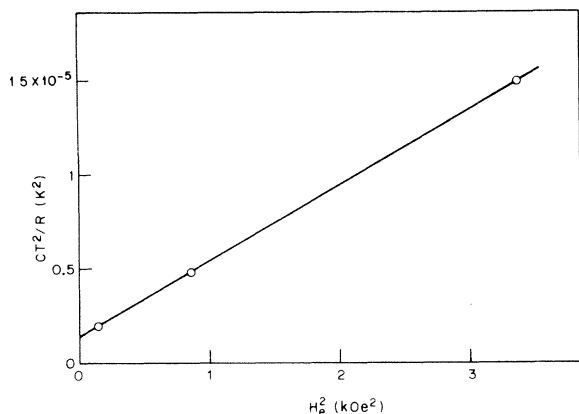


FIG. 12. Plot of CT^2/R against the square of the applied field.

course be of prime importance in order to decide whether or not the transition is of the second kind (in the thermodynamic sense), as expected if the nuclear ordering is of the cooperative kind. Figure 12 is a plot of C/RT^2 versus H_0^2 for 1836, 917, and 367 Oe. The straight line obtained confirms the approximate validity of Eq. (14). The slope yields a Curie constant of 3.36×10^{-4} emu K/mole, somewhat larger (19%) than the directly observed value of 2.84×10^{-4} emu K/mole. Within the limits of the validity of Eq. (14) then, the specific-heat data are thermodynamically consistent with the magnetization data. The straight line in Fig. 12 intercepts the abscissa at $H_0^2 = (534 \text{ Oe})^2$. This then is the external field that would (very approximately) simulate the observed (zero-field) specific heat in the ideal paramagnetic case (no ferromagnetic order). It is this value that has to be used in Eq. (8) for isentropic demagnetizations.

C. Thermal contact to the sample

In order to evaluate the usefulness of PrTl_3 as a paramagnetic cooling material, it is important to know the quality of the thermal contact that can be made to the sample.

Experimentally, we observe that when the sample is at 2.8 mK and we apply 6 erg/sec of heat flux into the two copper-wire strands (3 erg/sec into the upper strand and 3 erg/sec into the strand between the sample and the AuIn_2 thermometer), their temperature rises quickly to about 10 mK. Ideally, the contact between the copper cups and the PrTl_3 sample should be metallic, and there should be no Kapitza-type thermal boundary resistance. However, it is well known that rare-earth metals and intermetallic compounds can be wetted by soft solders (such as indium) without actually breaking the oxide layer and without making a good electronic contact. Since we have not

made electrical-contact-resistance measurements, we cannot rule out the existence of such a thin oxide layer. We therefore assume the existence of a Kapitza-type thermal boundary resistance between the copper cups and the PrTl_3 sample which dominates all other heat resistances, and write for the heat flow across the joint (R is the Kapitza resistance)

$$\dot{Q} = (1/R)A dt = aT^3 A dT$$

or

$$Q = \frac{1}{4} a A (T_H^4 - T_C^4)$$

(A is the surface area of contact equal to 0.5 cm^2 for both ends). The parameter a (which is equal to $1/RT^3$) would then come out to be

$$a = 4.8 \times 10^{-3} \text{ erg/cm}^2 \text{ sec mK}^4. \quad (16)$$

In nuclear-cooling experiments on PrCu_6 we found a value of $a = 6.9 \times 10^{-3}$ in the same units, i. e., the same order of magnitude. We estimate that this thermal resistance is only about five times larger than the thermal resistance of the copper-wire strands (between heaters and PrTl_3 sample) themselves. This suggests that we do have some electronic contact to our sample and that the assumption of a Kapitza-type boundary resistance [Eq. (15)] is probably too conservative. It is clear that the thermal contact to PrTl_3 is very much better than the one achieved between surfaces of conventional paramagnetic salts and metals, which is also of the form (15) with values of the parameter a between 10^{-6} and 10^{-7} erg/cm² mK⁴.¹⁴ PrTl_3 should be useful, for instance, to cool self-heating radioactive samples in nuclear-orientation experiments to low temperatures. If, for example, two such samples have self-heating rates of 1 and 0.1 erg/sec, one should be able to keep them initially below about 5.4 and 3.1 mK, respectively. The thermal conductivity of PrTl_3 at 1.7 mK is estimated to be about 0.11 mW/cm K, which in turn would mean that a steady heat flow of 0.1 erg/sec through one end of a cylindrical sample 0.56 cm in diameter would set up a temperature gradient of order 0.16 mK/cm.

V. SUMMARY

The nuclear-magnetic-susceptibility and nuclear-specific-heat measurements presented above confirm that PrTl_3 is a singlet-ground-state system with weak exchange interactions. The large enhancement of the nuclear Zeeman splitting in external applied fields is mainly a property of the individual ions and a consequence of their crystal-field and hyperfine interactions, as discussed before. The weak exchange interactions give rise to a critical parameter $\lambda\chi_{CF}$ (in molecular-field

notation) of 0.13, far from the value of 1 required for induced-moment order. PrTi_3 therefore represents a coupled electron-nuclear system which should exhibit cooperative nuclear order at very low temperatures as pointed out previously.¹³ The predicted ferromagnetic ordering temperature is 0.5 ± 0.17 mK, which compares favorably with the Curie-Weiss temperature of 1 ± 0.3 mK extrap-

olated from susceptibility data above 1.7 mK. Susceptibility and specific-heat data above this temperature are thermodynamically consistent. In spite of the observed thermodynamic irreversibility during demagnetization, which remains so far unexplained, PrTi_3 should prove to be a useful material to cool other metallic samples to temperatures as low as 1.6 mK.

¹K. Andres and E. Bucher, Phys. Rev. Lett. 21, 1221 (1968).

²K. Andres and E. Bucher, Phys. Rev. Lett. 22, 600 (1969).

³K. Andres and E. Bucher, Phys. Rev. Lett. 24, 1181 (1970).

⁴K. Andres, in *Proceedings of the 12th International Conference on Low Temperature Physics* (Keigaku, Tokyo, 1971), p. 641.

⁵K. Andres and E. Bucher, J. Appl. Phys. 42, 1522 (1971).

⁶K. Andres and E. Bucher, J. Low Temp. Phys. 9, 267 (1972).

⁷S. Darack, Bell Laboratories Technical Memorandum

No. 71-1114-11 (unpublished).

⁸K. Andres and J. H. Wernick, Rev. Sci. Instrum. 44, 1186 (1973).

⁹E. Bucher, K. Andres, J. P. Maita, A. S. Cooper, and L. D. Longinotti, J. Phys. (Paris) 32, C-1, 114 (1971).

¹⁰E. Bucher, J. P. Maita, and A. S. Cooper, Phys. Rev. B 6, 2709 (1972).

¹¹K. R. Lea, M. J. M. Leask, and W. P. Wolf, J. Phys. Chem. Solids 23, 1381 (1962).

¹²K. Andres, E. Bucher, S. Darack, and J. P. Maita, Phys. Rev. B 6, 2716 (1972).

¹³K. Andres, Phys. Rev. B 7, 4295 (1973).

¹⁴A. C. Anderson, G. L. Salinger, and J. C. Wheatley, Rev. Sci. Instrum. 32, 1110 (1961).